J. Aerosol Sci. Vol. 10, pp. 515 to 526.
© Pergamon Press Ltd. 1979. Printed in Great Britain.
0021-8502/79/0901-0515 $02.00/0

WATER DROPLET GROWTH MEASUREMENTS IN A CONTINUOUS FLOW PARALLEL PLATE THERMAL DIFFUSION CLOUD CHAMBER*

JAMES T. BROWN, JR. and F. D. SCHOWENGERDT
Department of Physics, Colorado School of Mines, Golden, CO 80401, U.S.A.

(*Received* 14 *July* 1978; *and in revised form* 7 *December* 1978 *and* 6 *March* 1979)

Abstract – A continuous flow thermal diffusion cloud chamber has been used to make real-time measurements of water droplet growth on a natural aerosol. Droplet size distributions were monitored with an optical particle detector. Droplet trajectories through the chamber were calculated in order to account for variations in the environmental conditions experienced by the growing droplets. The Fukuta–Walter droplet growth model has been used to predict droplet sizes along these trajectories. The results of the measurements and the predictions are compared and found to agree reasonably well using the commonly accepted values of 0.036 for the condensation coefficient and 1.00 for the thermal accommodation coefficient.

1. INTRODUCTION

As part of an effort to evaluate the utility of condensation enlargement to improve the control of respirable particulates, a continuous flow thermal diffusion cloud chamber was designed for the observation of water droplet growth by condensation. The chamber is a modification of one used earlier by Saxena and Fukuta (1974) in the study of the activation threshold for cloud condensation nuclei. Accounts of the evolution and applications of thermal diffusion cloud chambers are readily available (Mason, 1971; Saxena *et al.*, 1970).

The chamber, as adopted for use in the condensation enlargement experiments, allows a continuous variation of the saturation ratio and residence time within the chamber. The temperature is also variable but changes require substantial time delays since the characteristic thermal relaxation time for the system is of the order of hours. The geometry and operating conditions have been chosen so that end or edge effects as well as transient behavior may be evaluated and their perturbations minimized. In another article (Brown and Schowengerdt, 1979) we have analyzed the end and edge effects as well as the transient behavior in such a chamber.

A detailed description of the instrument is given in Section 2. In Section 3 we present the experimental procedures and an analysis of the experiment and in Section 4 the results of the growth rate measurements. In Section 5 the results are interpreted and compared with the Fukuta–Walter model for droplet growth and the conclusions are presented in Section 6.

2. EXPERIMENTAL SET-UP

Figure 1 is a schematic drawing of the diffusion cell in the continuous flow thermal diffusion cloud chamber. Because of the continuous range of supersaturations produced, it is often referred to as a spectrometer. It consists of three functionally different parts; the inlet chamber, the thermal circuit or diffusion cell, and the exhaust chamber.

The inlet chamber (not shown) is designed to provide for the uniform distribution of the pre-humidified carrier air over the cross-section of the diffusion cell and for the alignment of the injection probe through which the condensation nuclei and respirable particulates are injected into this air stream. Establishing a laminar-flow profile in as short a distance as possible is desirable and is aided by placing a diffuser near the inlet to the chamber. Any

* This project was supported by Grant No. Ro1 OH 00565-02 awarded by the National Institute of Occupational Safety and Health.

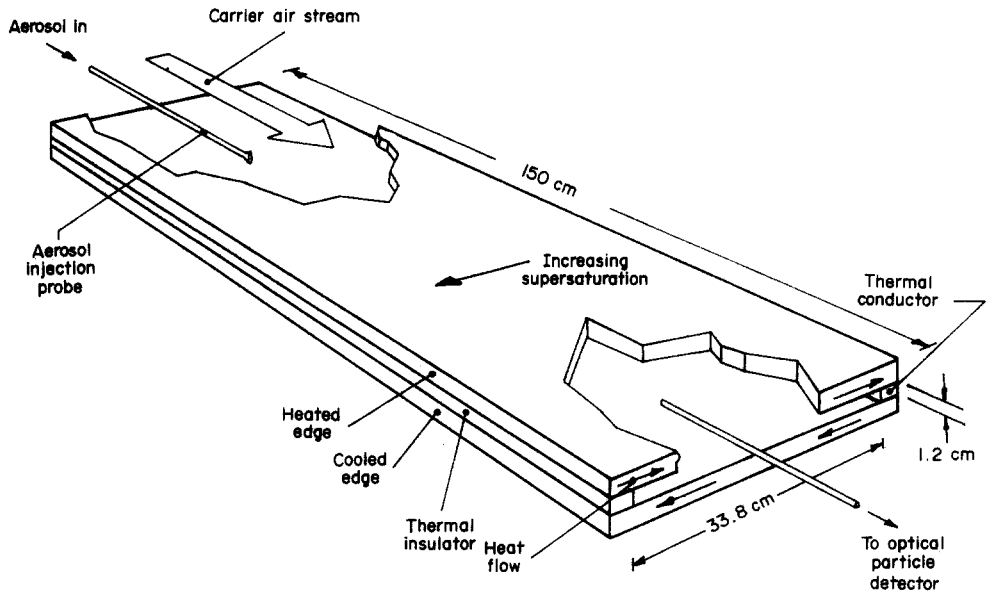

Fig. 1. A schematic diagram of the diffusion cell of the cloud chamber used for the droplet growth measurements. The inlet and exhaust chambers (not shown) are made of $\frac{1}{2}$ in. thick plastic and are fitted to the outside dimensions of the diffusion cell.

turbulence that might lead to mixing could add considerable uncertainty to the experiment; mixing in the vertical direction would be expected to modify the supersaturation profile and mixing in the horizontal direction would tend to destroy the resolution in supersaturation. The chamber also insulates the inlet end of the diffusion cell from heat losses.

The condensation nuclei are injected into the carrier air stream by means of a movable probe. The longitudinal position of the probe determines the residence time of the nuclei inside the diffusion chamber. The lateral position determines the supersaturation in which the droplets grow. The condensation nuclei are the naturally occurring particulates taken directly from the room air and fed to the probe through a metered fan.

It is in the diffusion cell where the supersaturated conditions are established and the

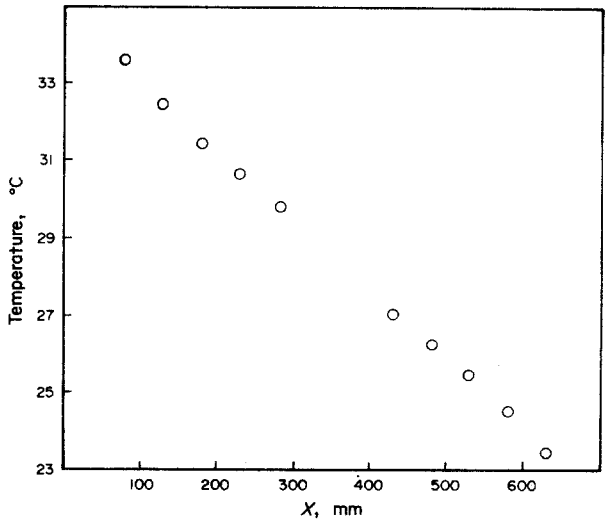

Fig. 2. A typical experimental temperature profile around the diffusion chamber where x measures the distance from the edge of the heated junction. $x = 688$ mm corresponds to the edge of the cooled junction. The saturation ratio may be calculated following the analysis of Brown and Schowengerdt (1979).

condensational growth takes place. The heated and cooled junctions (Fig. 1) which are separated by an insulating strip, establish an approximately linear thermal gradient across the conducting plates. Figure 2 shows a typical temperature profile where x is the distance from the heated junction measured across the top plate, through the conducting junction, and back across the bottom plate to the cooled junction. This "folded" thermal circuit results in a continuously variable thermal gradient across the gap between the plates. The gradient has a maximum of $(T_{hot}-T_{cold})/h$ (h is the plate separation) at the insulated junction and a minimum near zero at the conducting junction. The saturated boundary conditions which drive the diffusion of water vapor are maintained by the wetted canvas-covered inside surfaces of the chamber. The entire diffusion cell is insulated from its surroundings by a 5 cm layer of styrofoam.

The exhaust section is designed to maintain laminar flow at the exit and to insulate the outlet end of the system from heat losses. This end section also holds and aligns (with the inlet probe) a sampling tube which connects to the inlet of the particle detector and projects into the diffusion cell.

The thermally conducting plates of the diffusion cell are made of 1 in. thick aluminum. The temperature difference is maintained through the use of a heating tape imbedded in the edge of the top plate and the circulation of refrigerated water through the edge of the bottom plate. Small auxiliary heat tapes are attached along the length of the chamber to aid in eliminating longitudinal variations in the temperature. The temperature fields on both plates are measured by means of an array of 60 thermocouples which are mounted through the aluminum plates and project into the wetted canvas. The inlet and exhaust chambers are constructed of $\frac{1}{2}$ in. thick plexiglass and are fitted to the outside dimensions of the diffusion cell. To supply the carrier air, laboratory air is filtered, humidified to about 80% relative humidity and heated to near the midplane temperature of the diffusion cell.

An optical particle counter (Climet Instruments, Model 208, Redlands, California) is used to count and size the grown droplets. The output pulses are processed and stored in a multichannel analyzer (MCA) and droplet size data are obtained from it in the form of peak locations. The size distribution of the input condensation nuclei is monitored with an active scattering aerosol spectrometer (Particle Measuring Systems, Boulder, Colorado) and shows a maximum below 0.15 microns.

3. EXPERIMENTAL PROCEDURES AND ANALYSIS

In making the droplet growth measurements, the following procedure was used.

(a) Saturate internal surfaces of the diffusion cell repeatedly until thermal equilibrium is attained.
(b) Measure the equilibrium temperature profile over the region of interest within the chamber in order to determine the saturation ratio history for the growing droplets.
(c) Measure the carrier air velocity which is required to determine the residence or droplet growth time.
(d) Check input aerosol size distribution to insure that the initial nuclei sizes may be taken to be negligibly small.
(e) Calibrate the optical particle counter using latex spheres.
(f) Adjust the input aerosol flow to minimize effects due to moisture depletion.
(g) Set the inlet probe position (the distance between the inlet and sampling probe and the carrier air velocity determine the droplet growth time).
(h) Collect the droplet size spectrum on the MCA and determine the modal diameter, which is taken to be the characteristic size.
(i) Change the inlet probe position to vary the residence time and determine the corresponding droplet size as in (h). Typically this is done for 10–15 different residence times, each residence time being done twice; these measurements require up to 30 min.
(j) Remeasure the carrier air velocity to insure minimum variations in the residence time calculations.
(k) Remeasure the temperature profile to insure minimum variations in the saturation ratio

history of the growing droplets.

In order to analyze the experimental growth rate data it is necessary to accurately determine the following:

(a) the velocity of the carrier air,
(b) the temperature profile and the resulting supersaturation profile along the droplet trajectory,
(c) response characteristics of the particle detector,
(d) effects of moisture depletion,
(e) effects of sampling conditions, and
(f) the extent of transient and edge effects within the chamber.

Residence times of the growing droplets inside the chamber were inferred from measurements of the velocity of the carrier air stream. These velocities were determined through a series of time-of-flight measurements on pulses of smoke particles injected into the air stream. A schematic diagram of the time-of-flight system is shown in Fig. 3. In a typical velocity measurement smoke pulses were timed over a series of distances, a least squares fit of the time–distance data was made to a straight line, and the velocity was obtained from the slope of the best-fit line. A particular velocity determination was used only if the derived velocity varied less than about 1% from the measurements. It was determined that, within the range encountered in our experiments, the effects of smoke-pulse duration, injection pressure and droplet growth on the smoke, had minimal effects on the velocity measurements. A typical data set and least squares fit is shown in Fig. 4.

The temperature field within the chamber is monitored with an array of 60 copper constantan thermocouples; 30 were mounted on the inside of the top plate and thirty on the bottom, each projecting into the wetted canvas. Before being placed inside the chamber, each individual thermocouple was calibrated over a range of from 15 to 45°C. The resulting straight-line calibration curve for each one resulted in an accuracy of better than 0.1°C. No data were taken until all operating conditions within the chamber were stable to within the experimental resolution. This means that temperatures had to be constant to within 0.1°C in both time and in longitudinal position down the length of the cloud chamber. Achieving this constancy requires frequent rewetting of the internal canvas covered surfaces and adjustment of the auxiliary heating tapes.

Comparison of the experimental growth rates with the theoretical predictions (see Section 5) requires accurate knowledge of the entire temperature field. The parameter which is most sensitive to temperature variations is the saturation ratio S:

$$S = \rho(T)/\rho_{sat}(T), \tag{1}$$

where $\rho(T)$ is the actual water vapor density at the temperature T and $\rho_{sat}(T)$ is the saturated vapor density at the same temperature. In addition to the explicit temperature dependence in the theoretical model, several of the "constants" also show variations with temperatures.

The heights of the voltage pulses from the optical particle sensor are a function of the size and composition (index of refraction) of the particles being detected. For the present

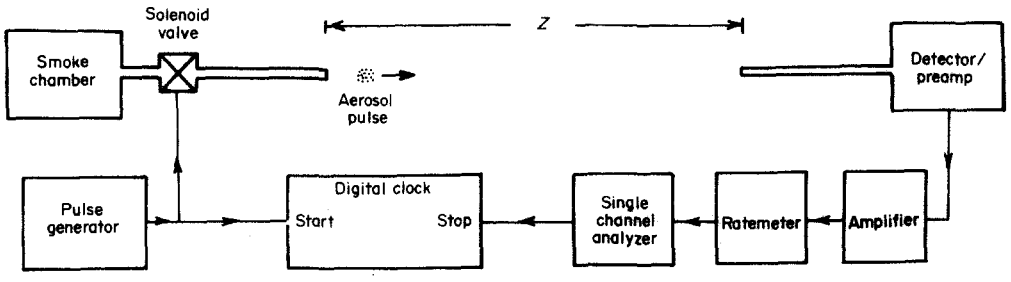

Fig. 3. A block diagram of the time-of-flight system used to determine the carrier air velocity in the cloud chamber.

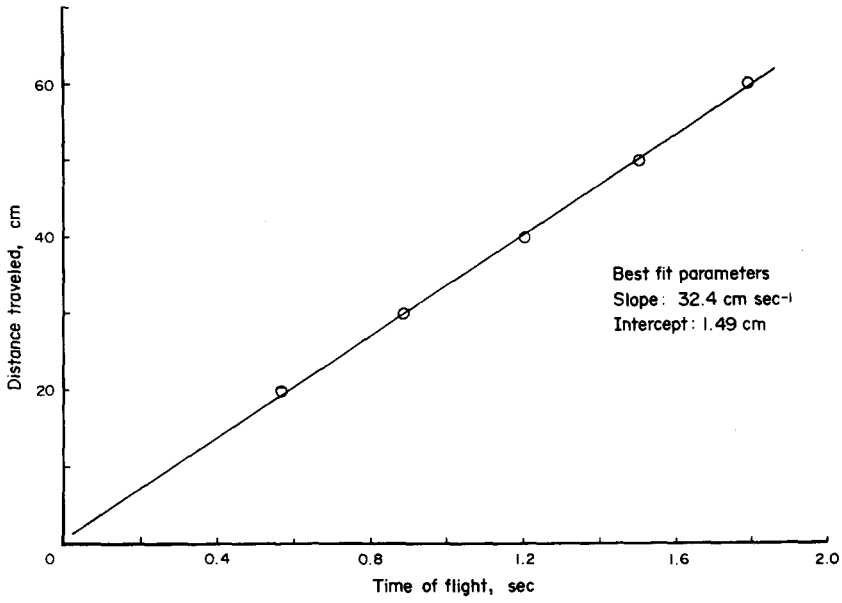

Fig. 4. A typical set of time-of-flight data (see Fig. 3) and the least squares linear fit; in this case the carrier air velocity is 32.4 cm sec^{-1}, which is the slope of the line.

experiment, the particle size scale was calibrated directly using commercially available latex spheres (Dow Chemical Company, Particle Information Services, Inc.). The spheres were aspirated and allowed to dry in a 150 ft^3 chamber before being used for calibration. Care was taken to avoid the well-known sources of error inherent in the use of aspirated latex spheres as standards (see, for example, *Aerosol Science*, 1966, Ch. 1, C. N. Davies, ed.).

The index of refraction for the latex spheres (~ 1.56) is different from that of water (~ 1.33) and may influence the interpretation of our data. The calculations of Cooke and Kerker (1975) applied to the characteristics of the Climet 208 detector indicate that a calibration based on the latex spheres may lead to undersizing of the water droplets by as much as 5% for the operating conditions of our detector and MCA. Since we have not been able to find experimental verification of these calculations for our instrument, although Tang *et al.* (1977) have obtained results for a modified Climet 208, we note this effect but do not include it in the calibration.

Droplet growth data were obtained as peak locations (modal diameters) displayed on the MCA in a droplet size spectra for a given residence time. In obtaining a given growth peak, several spectra were accumulated in order to ensure that equilibrium had been reached in the growing sample. During this time, the input aerosol concentration (condensation nuclei) was decreased until the peak location showed no more variation; this process ensures that moisture depletion does not interfere with the experiment. A qualitative comparison of effects due to moisture depletion and the associated supersaturation reduction with those predicted by Chodes *et al.* (1974) can be obtained by estimating the present droplet concentrations from the observed count rates. The latter were kept below 100 counts sec^{-1}, which when divided by the flow rate in the input aerosol beam gives about 36 droplets cm^{-3}. It should be noted that this is far below the 400 droplets cm^{-3} where Chodes *et al.* predicted a minimal effect in their apparatus.

Sampling conditions in the present experiment are far from isokinetic. Aerosol velocities are: $\gtrsim 40$ cm sec^{-1} in the chamber, $\sim 1.5 \times 10^3$ cm sec^{-1} in the sampling probe, and $\sim 1 \times 10^4$ cm sec^{-1} in the optical particle detector. First, it should be noted that these conditions do not produce the usual biasing of size distributions that is observed in many non-isokinetic sampling situations, because in the present case the aerosol traverses the chamber in a well-collimated beam. There are no aerosol particles outside this beam; thus, there is no possibility of pulling in particles of different sizes than would otherwise be present. There is, however, another possible effect: as the droplets are accelerated into the probe and

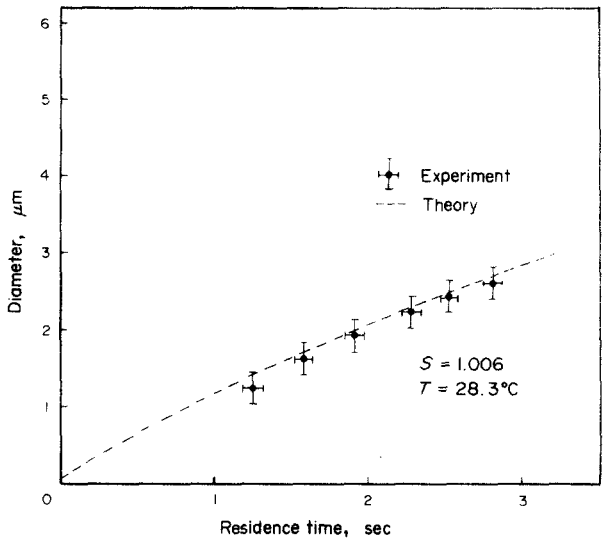

Fig. 5. The predictions of the Fukuta–Walter model are superimposed on the experimental water droplet growth data. The experimental droplet sizes are modal diameters with the full-width at half-maximum being the order of 15% of the diameter. The maximum saturation ratio was 1.006 and the midplane temperature was 28.3°C. The theoretical predictions are calculated for a droplet falling through the variable environment of the parallel diffusion cell (see Section 4) using a value of 0.036 for the condensation coefficient, 1.0 for the accommodation coefficient and 0.1 μm for the initial diameter.

detector, they experience a pressure drop and a resulting increase in supersaturation, which could produce additional growth. Given the aerosol velocities inside the probe and the detector, the corresponding pressure drops are 1.4 and 62 mbar, respectively. For a saturation ratio of 1.006, the first of these produces a saturation ratio in the probe of 1.024. However, since the droplets spend only 7 msec in this elevated supersaturation, the total time-averaged supersaturation increases negligibly. Inside the detector, the droplets cross the 1 cm distance from the inlet to the light beam in only 0.1 msec. The time-averaged increase in S here is also negligible.

In order to test the above assertions, growth rate measurements were made for sampling flow rates differing by a factor of 2. No appreciable change in the sizes of the detected droplets was observed. It was therefore concluded that, although the pressure drops are considerable, they have little effect on droplet growth in the present apparatus.

Transient and end effects which can significantly influence experiments in a continuous flow thermal diffusion cloud chamber include the following: transition from turbulent "plug flow" to laminar parabolic flow for the carrier air, evolution of equilibrium temperature and vapor density gradients from their uniform input state, and the development of the boundary layers along the edges of the chamber. An analysis of the equilibrium times for the sample introduced through the input probe indicates that, because of the velocities of interest and the size of the input probe orifice (about 2 mm), they may be neglected. Also, the temperature and relative humidity of the air which carries the condensation nuclei through the inlet probe were varied and there were no observable effects.

Fitzgerald (1970) and Saxena and Fowler (1973) have reported on the expected transients in supersaturation due to the different rates for approach to equilibrium of the temperature and diffusion fields. In an earlier article (Brown and Schowengerdt, 1979) we have analyzed the water vapor diffusion, heat conduction and fluid flow problems within the continuous flow cloud chamber. The conclusions of that analysis are the following.

(a) Laminar flow of the carrier air will be developed within the first 20 cm of travel between the plates. This result depends on velocity and applies for velocities less than 40 cm sec^{-1}.

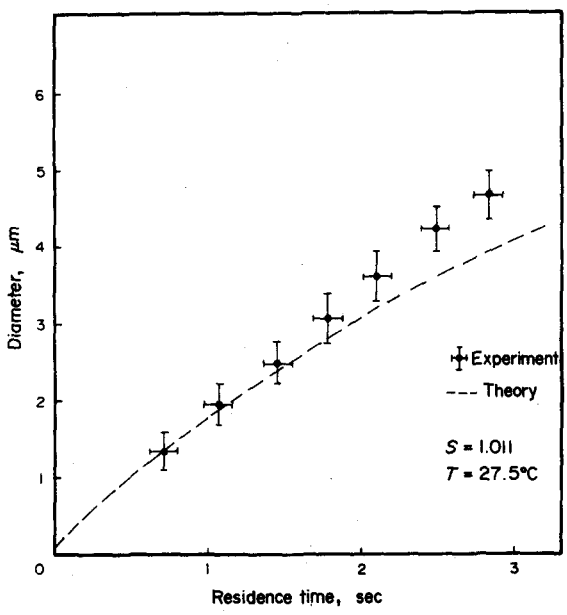

Fig. 6. Same as Fig. 5 except $S = 1.011$ and $T = 27.5°C$.

(b) The equilibration of the saturation profile, which is limited in time by the heat conduction process, will require about 1.0 sec and, therefore, takes place within the first 40 cm of the chamber for a carrier air velocity of 40 cm sec^{-1}.
(c) The numerical solution of the steady-state diffusion equation for the chamber shows that the edge effects, i.e. the spreading of water vapor isodensity contours, extend approximately 5 cm into the chamber from either side.
(d) After 150 cm of travel down the length of the chamber the side wall boundary layers will have evolved to about 2 cm from the walls.

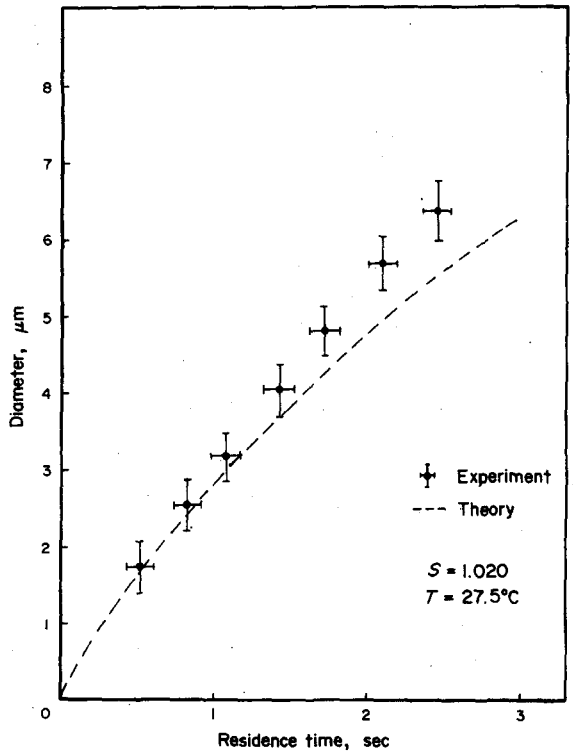

Fig. 7. Same as Fig. 5 except $S = 1.020$ and $T = 27.5°C$.

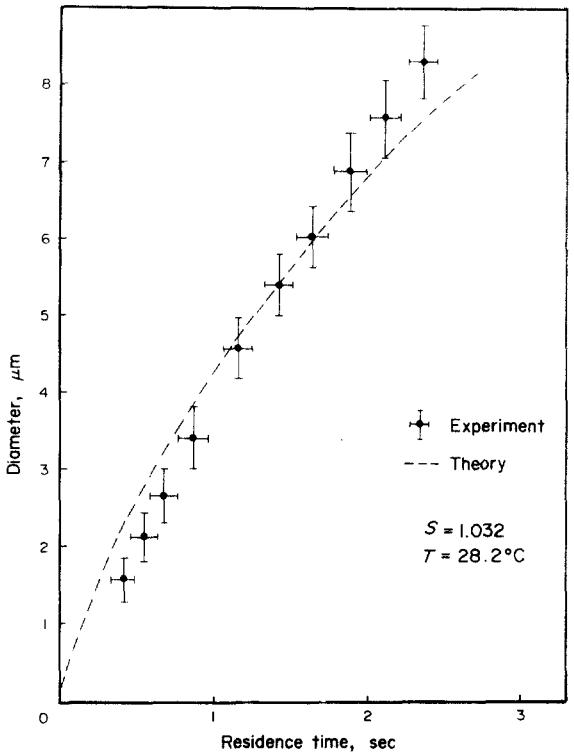

Fig. 8. Same as Fig. 5 except $S = 1.032$ and $T = 28.2°C$.

(e) If the experiments avoid the transient regions at the entrance to the chamber and the boundary layer along the two sides, steady state laminar flow conditions may be assumed to apply and the saturation ratios may be calculated from the local top and bottom plate temperatures assuming uniform temperatures on each plate.

4. EXPERIMENTAL RESULTS

Plots of the measured droplet diameters vs growth time are shown in Figs 5–8. Diameters were obtained as maxima in the final droplet size distributions as mentioned above. Each data point represents an average value of the results of at least four independent measurements. The error bars reflect the reproducibility of the data, together with estimates of uncertainties in the various experimental parameters to be discussed below. The broken lines included with the data are the predicted size-vs-growth-time curves obtained from the Fukuta–Walter model, as discussed below. Maximum saturation ratios, as calculated from the measured temperature using equation (1), are shown in the figures along with average values of the corresponding temperatures. The latter are accurate to 0.1°C, resulting in an uncertainty in $(S-1)$ of 11% in the worst case ($S = 1.006$), and 4% in the best case ($S = 1.032$). Carrier air velocities were about 40 cm sec^{-1}. The chamber was operated at atmospheric pressure, which in Golden, Colorado is about 63 cm Hg.

The theoretical prediction of the size-vs-growth-time for the droplets is obtained from the numerical integration of the Fukuta–Walter model. In order to carry out the integration, the environmental history of the droplet must be given for all times. In the continuous flow cloud chamber employed in these experiments, the droplets fall through both temperature and saturation ratio gradients. In addition, the velocity of the growing droplets varies according to the (laminar) parabolic velocity profile of the carrier air. The vertical (Stokes' law) velocity for the falling droplets also varies because of their increasing mass and size. We make the following assumptions in following the growing droplets.

(a) Stokes' law, including the Cunningham correction, is taken to describe the fall of the droplets, i.e. they are assumed to be falling at the appropriate terminal velocity $v_{\text{Stokes}}(r)$ (calculation of the relaxation time justifies this assumption).
(b) The saturation ratio is given by:

$$S(y) = \frac{\rho(y)}{\rho_{\text{sat}}(T(y))},$$

where $\rho(y)$ is the water vapor density predicted from the one-dimensional steady-state diffusion equation, $\rho_{\text{sat}}(T(y))$ is the saturation vapor density at the temperature T and T is assumed to vary linearly with the vertical position, y, within the chamber (numerical integration of the conduction and diffusion equations has justified this assumption).
(c) Laminar flow and the parabolic velocity profile $v(y)$ across the height of the chamber exists. (See Brown and Schowengerdt, 1979.)
(d) Diffusio- and thermo-phoresis may be neglected. Our estimates indicate that they will, in the worst case, contribute an integrated effect of less than 0.5 mm to the total vertical displacement.

The position, environment and size of the droplets is evolved according to the following algorithm.
(a) The condensation nucleus is injected into the chamber at a given vertical position, y.
(b) The droplet grows for an interval Δt at the appropriate saturation ratio $S(y)$.
(c) The droplet moves a distance $v(y)\Delta t$ along the length of the chamber.
(d) The droplet falls a distance $v_{\text{Stokes}}(r)\Delta t$.
(e) The resulting position changes are used to iterate steps (b), (c) and (d).

The numerical analysis of the droplet trajectories reveals an interesting result: the effects due to the parabolic velocity profile are very nearly canceled by the saturation ratio profile. While not truly parabolic, the saturation ratio variation from the top to the bottom of the chamber can be approximated well by such a function. The conclusion from this observation is that a very good estimate of the variable conditions within the instrument can be obtained by treating the velocity and saturation ratio as constants equal to their respective maximum values.

A typical set of trajectories is shown in Fig. 9 and the saturation ratio histories to which the droplets are exposed as they follow the various trajectories are shown in Fig. 10. Figures 9 and 10 are both for the case where the maximum saturation ratio is 1.020 and the carrier air velocity is 40 cm sec^{-1}.

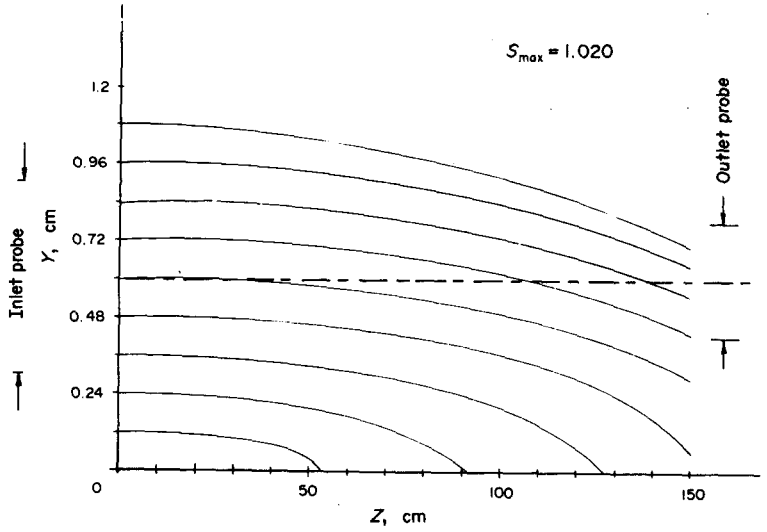

Fig. 9. The trajectories (vertical position vs travel distance along the chamber) of growing droplets for various initial vertical positions. $y = 1.2$ cm corresponds to the top of the chamber, $y = 0$ cm to the bottom. $z = 0$ cm the inlet.

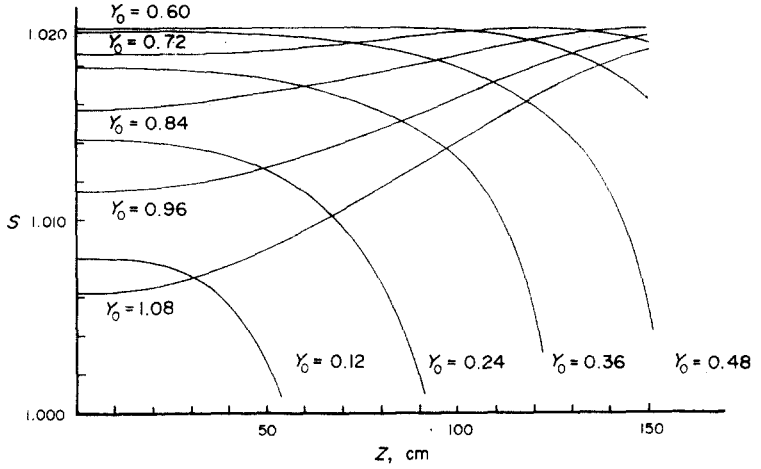

Fig. 10. The saturation ratio trajectory (or history) of the growing droplets as they travel the length of the diffusion cell. Since the local saturation ratio depends on the vertical position between the plates as the droplets grow and fall they experience a varying saturation ratio.

5. INTERPRETATION OF THE RESULTS

The zeroth-order Maxwell description of the growth of a water droplet due to condensation is presented in detail by Mason (1971) and Byers (1965). In the Maxwell model it is assumed that the diffusion and temperature fields are in a steady state, that the water vapor may be described as an ideal gas and that the Clausius–Clapeyron equation gives the temperature dependence of the vapor pressure during the phase change (condensation). The resulting non-linear differential equation may be integrated to yield

$$r^2 = r_0^2 + \frac{2(S-1)t}{a+b},$$

where a, b are constants and S is saturation ratio, which provides a good description for droplets with r_0 of the order of tens of microns.

Fukuta and Walter (1970) and Carstens and Carter (1974) present a chronologically ordered discussion of the efforts to generalize Maxwell's theory, particularly to include the description of smaller droplets (also see *Physics of Drop Formation in the Atmosphere*, Sedunov, 1972). In general terms, this extension to smaller sizes requires a microscopic or "kinetic" level examination of the thermal and mass transport processes within approximately one mean-free path of the surface of the droplet. Fukuta and Walter introduce scale factors $f_{3\alpha}$ and $f_{3\beta}$ which measure the deviations of the Knudsen flow from the Maxwell prediction. The resulting differential equation describing the growth of the droplet is:

$$\frac{d(r^2)}{dt} = \frac{2(S-1)}{a/f_{3\alpha} + b/f_{3\beta}}.$$

The definition of $f_{3\alpha}$ and $f_{3\beta}$ contain implicit dependence on the droplet size, r, the accommodation coefficient α and the condensation coefficient β; the explicit definition of these variables is found in the original paper (Fukuta and Walter 1970). α and β are generally treated as parameters to be determined by experiment. When important, curvature and solution effects may be incorporated into the model and the form of the growth equation remains the same with the changes showing up as a modification of the terms containg a and b. The size of the growing droplet as a function of time as predicted by this model is smaller for all times than that predicted by the Maxwell equation.

In making comparisons between the present experimental results and the work of others, it should be kept in mind that the purpose of the present apparatus is to provide reliable, real-

time, growth data in a routine manner. On the other hand, most of the growth (and evaporation) experiments have had as their objectives precise one-time measurements of certain theoretically significant parameters. Of these, the most often measured is the condensation coefficient, β. This coefficient, which is the fraction of the incident water molecules which stick to the droplet (sticking probability), appears in all the current theories. Its measurement, therefore, provides a convenient standard by which to judge the reliability of the present growth apparatus. The thermal accommodation coefficient α (ratio of thermal energy transferred to maximum possible transfer) is normally found to be close to unity.

Reviews of experimental determinations of β are to be found in the works of many authors (see Sinnarwalla *et al.*, 1975, for example). Apparently one of the earliest experiments (Alty and Mackay, 1935), in which the value $\beta = 0.036$ was obtained, is the most widely referenced, having produced a result which is very close to the average of most of the modern experiments. Alty and Mackay's results were obtained by observing the evaporation of drops formed on a glass tip. Duguid and Stampfer (1971) measured evaporation rates of much smaller (3–9 μm radius) droplets and concluded that the evaporation coefficient (equal to β) had to be at least 0.5 in order to fit the data. Chodes *et al.* (1974) have pointed out two problems with the results of Duguid and Stampfer, namely, unaccounted for scatter in the data and inference from the data of a finite evaporation rate for saturated conditions.

Recent growth measurements have been done by Vietti and Schuster (1973), Chodes *et al.* (1974), Gollub *et al.* (1974) and Sinnarwalla *et al.* (1975).

Vietti and Schuster (1973) have measured growth rates on water droplets of radius 0.45–10 μm in a Wilson cloud chamber. Saturation ratios ranged from 1.49 to 3.45. Droplet size was deduced from measured oscillations in the intensity of polarized laser light scattered to 30°. With β constrained to 0.035 their data required an unrealistically low value of $\alpha = 0.1$ for a good fit to the Fukuta–Walter theory. A formulation of Schuster produced an overall better fit when the sticking coefficient was set equal to 0.21. However, Carstens and Carter (1974) have repeated their measurements using the same apparatus and found a value of $\beta = 0.03$ for $\alpha = 1.0$.

Chodes *et al.* (1974) measured growth rates on droplets smaller than 3 μm at saturation ratios of 1.0040–1.0072 in a thermal diffusion cloud chamber. The growth of 40 individual droplets was observed and recorded photographically. On the assumption that $\alpha = 1.0$, they obtained an average value of 0.033 with a standard deviation of 0.005 for β.

Gollub *et al.* (1974) measured droplet growth rates for supersaturations of 1.01–1.05 in the size range 3–7 μm. Droplet size distributions were obtained from heterodyne spectra of scattered laser light. The authors find a good fit to their data for $\alpha = 1.0$ and $\beta = 0.12$ in contrast to the much lower values of β found necessary to fit data of others at higher supersaturations.

Sinnarwalla *et al.* (1975) measured growth rates on droplets smaller than 7.5 μm at saturation ratios of 1.005 and 1.01 using a vertical flow thermal diffusion cloud chamber. Essentially, their method was to measure the terminal gravitational settling velocity photographically, then calculate the radius on the basis of Stokes' law. The resulting values of β ranged from 0.021 to 0.032 with probable errors from -12.5 to 9.5%.

In other studies (see Sinnarwalla *et al.*, 1975), values for β ranging from 0.006 to 0.42 have been found. Several possible explanations for this wide variation in experimental results have been advanced. These include: variations in the amounts of hygroscopic material in the test aerosol, contaminants in the water, time dependence of β and ventilation effects (replenishment of the moisture supply to the growing droplet by virtue of its motion through the vapor). Ventilation effects have been addressed by Squires (1952), who found that they could be neglected for droplets smaller than about 10 μm in radius. Davies (see Shaw 1978, Chapter 3) has shown that ventilation is expected to have an effect of less than 3% for droplets smaller than 10 μm.

Because of this apparent disagreement between various experiments, comparisons should be made with due regard to differences in experimental methods and conditions. For want o a better value of β, we have taken $\beta = 0.036$, for use in the growth calculations shown in Figs 5–8.

6. CONCLUSIONS

The agreement between theory (with $\alpha = 1.0$ and $\beta = 0.036$) and experiment shown in Figs 5–8 is quite good; the maximum disagreement in any of the curves is about 15%. There is, however, a clear indication of a small systematic disagreement in the slopes of the curves. Using the Fukuta–Walter model as incorporated into the trajectory algorithm discussed in Section 4, the best fit to the data is obtained with a value of 0.07 for β ($\alpha = 1.0$), but because the determination of this parameter was not the object of the experiment, we choose not to emphasize this number.

For purposes of establishing the reliability of the present method, the agreement with theory and previous experiments can be considered good. In view of this agreement in the case of naturally occurring nuclei, we conclude that the method can be used with some confidence on respirable mineral particulates. However, care must be taken to account for the content of hygroscopic material in the nuclei and for the surface activity, relative to water vapor, of the particulates. Variations in the characteristic nucleation times of the nuclei may be observable as a shift in the time axis of the growth curves. The available resolution in size and residence time for the experimental arrangement used here appears to permit the study of techniques to modify the nucleation and growth rates for water droplets on arbitrary nuclei.

Acknowledgements – We wish to acknowledge Messers Mark Albers, Tony Applehans, Richard Fellion and Richard Mitchell for their assistance in performing the experiments and the additional financial support of Atlantic Richfield Co., Bear Coal Co., Colorado Fuel and Iron, Public Service Company of Colorado and U.S. Steel.

REFERENCES

Alty, T. and MacKay, C. A. (1935) *Proc. R. Soc.* **A149,** 104.
Brown, J. T. and Schowengerdt, F. D. (1979) *J. Aerosol Sci.* **10,** 339.
Byers, H. R. (1965), *Elements of Cloud Physics*, The University of Chicago Press, Chicago and London.
Carstens, J. C. and Carter, J. M. (1974), Current Meteorological Theory of Drop Growth by Condensation and Some Comparisons with Experiments, *Proc. Int. Conf. on Drops and Bubbles*, Cal-Tech-J.P.L., August.
Chodes, N., Warner, J. and Gagin, A. (1974) *J. Atmos. Sci.* **31,** 1351.
Cooke, D. D. and Kerker, M. (1975) *Appl. Opt.* **14,** 734.
Davies, C. N., editor (1966) *Aerosol Science*, Academic Press, London and New York.
Duguid, H. A. and Stampfer, J. F., Jr. (1971) *J. Atmos. Sci.* **28,** 1233.
Fitzgerald, J. W. (1970) *J. Atmos. Sci.* **27,** 70.
Fukuta, N. and Walter, N. A. (1970) *J. Atmos. Sci.* **27,** 1160.
Gollub, J. P., Chabay, Ilan and Flygare, W. H. (1974), *J. chem. Phys.* **61,** 2139.
Mason, B. J. (1971) *The Physics of Clouds*, Clarendon Press, Oxford, 2nd edition.
Saxena, V. K., Burford, J. N. and Kassner, J. L. (1970) *J. Atmos. Sci.* **27,** 73.
Saxena, V. K. and Fowler, J. L. (1973) *J. appl. Meteorol.* **12,** 984.
Saxena, V. K. and Fukuta, N. (12/1974), Cloud Condensation Nucleus Spectrometer, Denver Research Institute Report No. 2657, University of Denver.
Sedunov, Y. S. (1972) *Physics of Drop Formation in the Atmosphere*, Halsted Press, Wiley, New York.
Shaw, D. T., editor (1978) *Fundamentals of Aerosol Science*, Wiley, New York.
Sinnarwalla, A. M., Alofs, D. J. and Carstens, J. C. (1975) *J. Atmos. Sci.* **32,** 592.
Squires, P. (1952) *Aust. J. Sci. Research* **A5,** 59.
Tang, I. N., Munkelwitz, H. R. and Davis, J. G. (1977) *J. Aerosol Sci.* **8,** 119.
Vietti, M. A. and Schuster, B. G. (1973) *J. chem. Phys.* **58,** 434.